Angewandte Chemie

Nanocluster Catalysts

Benzene Formation at 70 °C by Coupling of Propylene on Supported Pd Nanoclusters**

*Ju Chou, Siyan Zhang, Shouli Sun, and Eric W. McFarland**

Reactions on supported transition metal clusters have important applications and often display unexpected reactivity when the cluster size is on the nanometer scale.[1] As reliable methods of preparing size-selected supported clusters have been developed, relationships between the preparation method, size, and/or support have become apparent, albeit poorly understood. Metal clusters can be synthesized by using micelle encapsulation, and this method has been further developed to make nanocluster powders supported on metal oxides.[2–4] The metal ions are initially dissolved homogeneously within the hydrophilic block copolymer cores of the micelle solutions, and the length and structure of the copolymers can be used to control the sizes of the clusters.[3,5] A uniform distribution of metal nanoclusters is created throughout the polymer matrix[5] and in the resulting powder catalyst.

Supported Pd clusters on metal oxides are widely used as industrial heterogeneous catalysts.[6] They are known catalysts for the hydrogenation of olefins,[7] propylene epoxidation,[8–9] and the production of hydrogen peroxide.[10] Coupling or cyclization of the alkynes acetylene[11–14] and propyne[15–16] has also been observed. The cyclotrimerization of acetylene on Pd deposited on MgO thin films or W surfaces was observed to occur at 330 K and higher, and was found to be dependent on the size and coverage of Pd nanoclusters. This coupling reaction leads to the formation of benzene through C activation on the Pd surface and end-to-end C–C coupling. Propyne has also been observed to couple to benzene on a Cu surface at 260 K in an ultra high vacuum (UHV) system.

---

[*] Dr. J. Chou
Department of Chemistry and Physics
Southeastern Louisiana University
Hammond, LA, 70402 (USA)

Dr. S. Sun, Prof. E. W. McFarland
Gas Research Technology, Inc.
861 Ward Drive, Santa Barbara, CA 93111 (USA)
Fax: (+1) 805-893-4731
E-mail: mcfar@engineering.ucsb.edu

S. Zhang, Prof. E. W. McFarland
Department of Chemical Engineering
University of California
Santa Barbara, CA, 93106-5080 (USA)

[**] The authors are grateful for financial support from the U.S. Department of Energy (DE-FG03-89ER14048), the U.S. Air Force Office of Scientific Research (DURINT grant F49620-01-1-0459), and the National Science Foundation (CHE-9626338). The authors thank Professor Galen Stucky and Professor Horia Metiu for helpful discussions, and Dr. Tom Mates and Dr. Jinping Zhang for technical assistance with XPS and TEM. The authors made use of the MRL Central Facilities, supported by the MRSEC Program of the NSF under Award DMR-00-80034.

DOI: 10.1002/ange.200500022

Head-to-tail interaction of two propyne molecules takes place to produce benzene with the elimination of hydrogen.[16] Though observations of propylene coupling to form aromatic compounds on acid or bifunctional catalysts has been previously observed, these have all been attributed to radical processes that require high temperatures (> 300 °C).[17] To our knowledge, there are as yet no reports of propylene coupling to benzene on supported metal catalysts at low temperature.

In our previous investigations of propylene partial oxidation (epoxidation) on supported Au in the presence of hydrogen and oxygen, we observed traces of benzene while using Au–Pd alloys. With an increased Pd/Au ratio we observed an increase in the rate of benzene production. Herein, we describe our subsequent follow-up to the preliminary observations in which we addressed the following questions: what are the conditions under which Pd clusters supported on TiO_2 can catalyze propylene coupling to produce benzene? Is the propylene coupling reaction size-dependent? What is the mechanism involved in the formation of benzene from propylene coupling?

Three Pd nanocluster sizes were prepared in micelles of three different block copolymers respectively and supported on TiO_2 by impregnation. The powders were dried and calcined at 300 °C. The calcination procedure removed the polymer surrounding the metal cluster (observed by MS, $M_r = 44$) and partially reduced Pd^{II} to metallic Pd^0. The calcination was followed by treatment with hydrogen at 250 °C to complete the reduction of Pd^{II} to Pd^0. The final powder catalysts, Pd/TiO_2, were characterized by HRTEM (Figure 1).

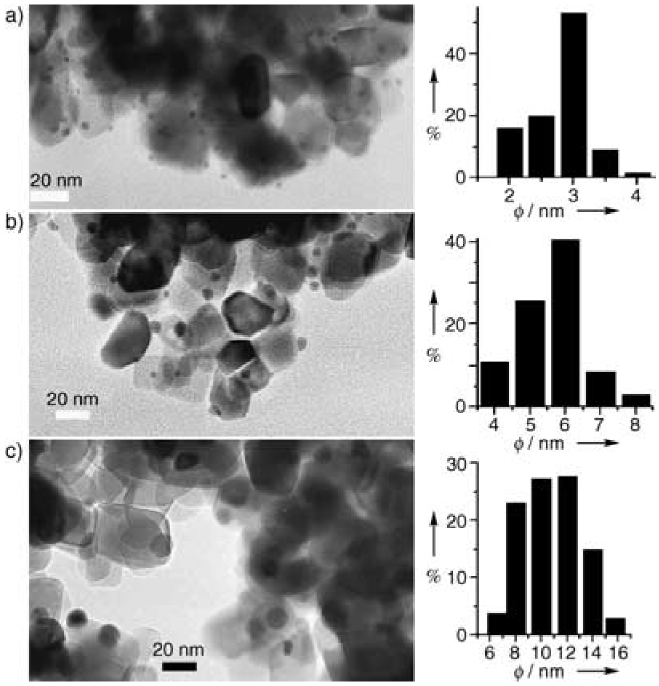

Figure 1. TEM images (left) of Pd nanoparticles prepared on titania supports from polymers with three different head sizes after calcination and reduction. Histograms (right) show the corresponding Pd size distributions obtained for: a) PS(54300)-P2VP(8800), $\varnothing = 3 \pm 1$ nm; b) PS(81000)-P2VP(14200), $\varnothing = 6 \pm 2$ nm; c) PS(53000)-P2VP(43800), $\varnothing = 12 \pm 3$ nm.

The micrographs and corresponding histograms show Pd nanoclusters uniformly dispersed on TiO_2 with a narrow size distribution. The diameters of the nanoclusters from the three different polymers were determined by HRTEM to be 3 ± 1, 6 ± 2, and 12 ± 3 nm.

X-ray photoelectron spectra (XPS) were collected with the Pd/TiO_2 catalyst to determine the Pd oxidation states before and after calcination, after reduction in hydrogen, and after the reaction. Figure 2 shows the measured Pd 3d core-level spectra of the Pd/TiO_2 ($\varnothing = 6$ nm). While still surrounded by the polymer micelle before calcination, the binding energy (E_b) of the Pd catalyst is observed as two broad peaks which are thought to be the superposition of two pairs of peaks at $E_b = 336.3$ and 341.6 eV, and at $E_b = 338.1$ and 343.3 eV. The former pair is assigned to PdO[10] and the latter ($E_b = 338.1$ and 343.3 eV) we believe corresponds to Pd^{II} bound to the CH_3COO- groups of the micelle. Both peaks are consistent with Pd^{II}.

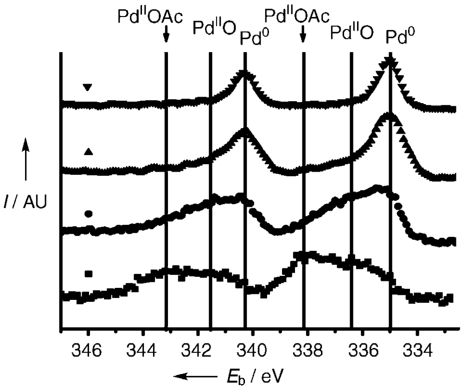

Figure 2. XPS of the Pd 3d region of the Pd/TiO_2 catalyst before calcinations (■), after calcinations (●), after reduction in hydrogen (▲), and after propylene reaction (▼).

After calcination the binding energy decreases, and two chemical states of Pd are observed. Peaks at 336.3 and 341.6 eV are still assigned to $Pd^{II}O$; however, the peaks at 335.0 and 340.3 eV are attributed to Pd^0.[18] Therefore, calcination partially reduces palladium(II) and removes the measurable polymer surrounding Pd. After reduction in hydrogen, the major peaks are at 335.0 and 340.3 eV which arise from Pd^0; a small tail of $Pd^{II}O$ remains, however.

The activity of Pd/TiO_2 in a mixture of propylene, hydrogen, and oxygen was measured in a packed bed reactor with argon as a carrier and calibration standard. The mixture was controlled by a mass flow controller at 2 mL min^{-1} for each gas with a total flow rate of 8 mL min^{-1}. The reaction products were analyzed by MS, GC, and ^{1}H NMR spectroscopy.[4,19]

Figure 3 shows the products of the reaction of propylene, hydrogen, and oxygen on Pd/TiO_2 as measured by on-line MS during a temperature increase at a rate of 2.5 °C min^{-1}. At approximately 70 °C, a rapid increase in benzene production ($M_r = 78$) was observed as well as increases in the production of species with $M_r = 44$ (CO_2 and C_3H_8), $M_r = 43$ (C_3H_8), and $M_r = 58$ (C_3H_6O). The masses of both CO_2 and C_3H_8 are 44;

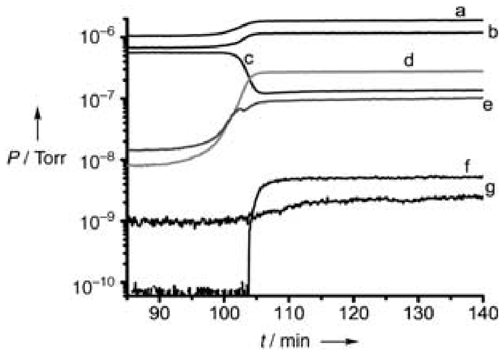

Figure 3. On-line MS data from the reaction of propylene, hydrogen, and oxygen on Pd/TiO_2 ($\varnothing = 3$ nm) as the catalyst temperature is increased from room temperature to 70 °C. Species shown and their corresponding M_r values are: a) Ar, 40; b) C_3H_6, 42; c) O_2, 32; d) ($CO_2 + C_3H_8$), 44; e) C_3H_8, 43; f) C_6H_6, 78; g) C_3H_6O, 58.

however, C_3H_8 has a unique fragment at $M_r = 43$. Therefore, the change in $M_r = 44$ results from the presence of both CO_2 and C_3H_8, whereas the signal at $M_r = 43$ is solely that of C_3H_8. The signal at $M_r = 58$ is also ambiguous and could be from the isomers acetone, propanal, or propylene oxide.

Further identification of each product was confirmed by both GC and NMR spectroscopy. On-line GC analysis shows that the products include CO_2, acetone, propane, and benzene. Finally, the reaction products were collected by a cold trap of $CDCl_3$. Figure 4 shows the ^1H NMR spectrum of collected products. The chemical shift at $\delta = 7.4$ ppm is that of benzene. Propane and acetone were also observed in the NMR spectrum (Figure 4), which is in good agreement with our analysis of the GC and MS results. For all cases in which benzene was formed, we observed that it is preceded by oxidation and hydrogenation, and is accompanied by the condensation of water at the reactor outlet.

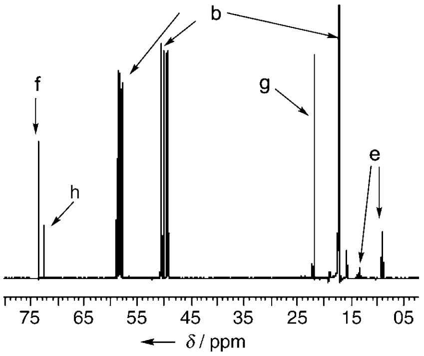

Figure 4. ^1H NMR spectrum of the products of the catalytic reaction at 25 °C on Pd/TiO_2 ($\varnothing = 3$ nm). The peaks are assigned to b) C_3H_6; e) C_3H_8; f) C_6H_6; g) C_3H_6O (acetone); h) $CDCl_3$.

The activities of the different Pd nanocluster sizes on TiO_2 were determined, and Table 1 shows product conversion and selectivity as a function of nanocluster size at 70 °C. Under the same experimental conditions, the 3-nm diameter Pd clusters were the most active. The selectivity for deep oxidation to carbon dioxide is inhibited on the smallest clusters, which favor hydrogenation, coupling, and partial oxidation. As a control, large (bulk) Pd clusters were prepared by sintering the powder catalyst to 1000 °C. The large cluster sizes were confirmed by SEM and were inactive for propylene coupling to form benzene at 70 °C; the only observed products in this case were propane and acetone.

Table 1: Performance of TiO_2-supported Pd nanoclusters ($\approx 1\%$ by weight) of different sizes for the reaction of a mixture of propylene, hydrogen and oxygen.

Pd Size [nm]	T [°C]	Selectivity [%]				Conversion C_3H_6 [%]
		Benzene	Acetone	Propane	CO_2	
3	70[a]	4.9	1.7	69.5	23.9	20.3
6	70[a]	4.2	0.7	36.5	58.6	12.0
6	70[b]	4.3	0.9	19.8	75.0	33.5
12	70[a]	2.5	0.4	31.1	66.0	11.4

Reactant gas molar ratios: [a] $Ar/O_2/H_2/C_3H_6 = 2{:}2{:}2{:}2$. [b] $Ar/O_2/H_2/C_3H_6 = 1{:}3{:}2{:}2$.

After reaction, XPS analysis of the catalyst shows the presence of only Pd^0. To test the hypothesis that Pd^0 is required for the formation of benzene, the reaction was carried out with a Pd catalyst lacking prior reduction, leaving $Pd^{II}O$ on the surface. Under the same reaction conditions as above, benzene formation was not observed, which suggests that metallic Pd^0 is necessary for the formation of benzene.

The production of benzene requires the co-reactants oxygen and hydrogen; on Pd/TiO_2 ($\varnothing = 3$ nm) in the presence of both oxygen and hydrogen ($O_2/H_2/C_3H_6 = 2{:}2{:}2$ mL min^{-1}), benzene formation was observed. Upon replacement of hydrogen with Ar to maintain the total flow rate at 6 mL min^{-1} ($Ar/O_2/C_3H_6 = 2{:}2{:}2$ mL min^{-1}), the production of benzene and all other products (CO_2, propane, and acetone) stopped. No activity was observed at 70 °C without hydrogen.

When oxygen was absent, not surprisingly, oxidation of propylene to CO_2 and acetone stopped; however, hydrogenation to propane was observed by both MS and NMR spectroscopy. Upon returning to the original flow rates of propylene, oxygen, and hydrogen (2:2:2 mL min^{-1}) on the same catalyst, the formation of benzene was again observed.

These observations indicate that both oxygen and hydrogen are required for the production of benzene at low temperatures on the Pd clusters. The product reactions are summarized in Equations (1)–(4) :

$$H_3C{-}CH{=}CH_2 + H_2 \rightarrow H_3C{-}CH_2{-}CH_3 \tag{1}$$

$$H_3C{-}CH{=}CH_2 + O_2 + H_2 \rightarrow (H_3C)_2{-}C{=}O + H_2O \tag{2}$$

$$H_3C{-}CH{=}CH_2 + 5\,O_2 + H_2 \rightarrow 3\,CO_2 + 4\,H_2O \tag{3}$$

$$H_3C{-}CH{=}CH_2 + O_2 + \frac{1}{2}\,H_2 \rightarrow \frac{1}{2}\,C_6H_6 + 2\,H_2O \tag{4}$$

For the reaction of propylene to produce benzene we tentatively propose a mechanism on the Pd cluster surface that involves H-atom abstraction that initially couples two propylene molecules. This is energetically driven by the formation of water with C–H bond activation through an activated intermediate of the hydrogen/oxygen reaction. Figure 5 illustrates the proposed reaction cycle. The observation that benzene formation from propylene is preceded by hydrogenation and oxidation suggests that the Pd surface is populated by hydroxy and/or peroxide species that result from the dissociative chemisorption of hydrogen and oxygen.[10,20] These species abstract a hydrogen atom from the terminal methyl group of a π-bound propylene molecule on the surface. This initial hydrogen abstraction produces a symmetric allyl intermediate[21] which then cyclizes with an adjacent allyl group to form the cyclic intermediate **I** and water. Although it is known that on a bifunctional catalyst, two allyl groups can couple to form 1,5-hexadiene as a by-product and benzene by dehydrogenation, 1,5-hexadiene products were not observed by MS. Thus, in the low-temperature Pd-catalyzed propylene coupling reaction, the cyclization apparently does not follow the conventional mechanism via 1,5-hexadiene; instead, it may proceed to form intermediate **I** (Figure 5). The mechanism of propyne coupling to form benzene via cyclohexadiene intermediates has been proposed.[16] The formation of water provides the energetic drive necessary for the removal of hydrogen. The fact that Pd nanoclusters are required for efficient low-temperature coupling suggests that either the very low coordination (giving rise to the suggested structures analogous to bis(allyl)palladium complexes) and/or surface intermediates that are sufficiently different from the pure metal (or metal–ligand complexes previously studied) are responsible for this unusual reactivity.

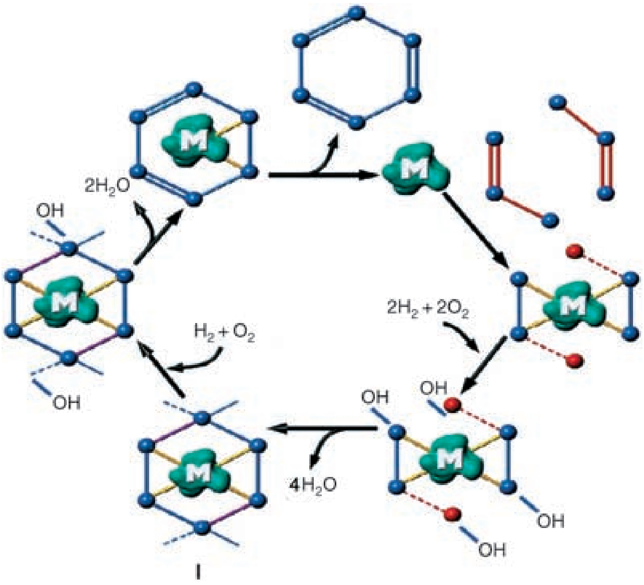

Figure 5. Mechanism of propylene coupling, leading to the formation of benzene. M represents one or more metal sites.

Experimental Section

Block copolymers of poly(styrene)–block–poly(2-vinylpyridine) (PS-b-P2VP) of three molecular weights were used to make Pd micelle solutions.[3,17] Pd/TiO$_2$ catalysts were prepared by using Pd acetate with the following procedure: 50 mg block copolymer PS(x)-b-P2VP(y) (54300/8800, 81000/14200, 54000/43800, Polymer Source, Inc., Canada) was dissolved in toluene (10 mL) and stirred for 5 h. This was followed by the addition of 20 mg Pd acetate (or 16 mg for 3-nm diameter Pd) into the solution and continuous stirring for 48 h. The different Pd nanocluster sizes were obtained by changing the length of the polymer head (PS). The Pd micelle precursors were then deposited onto anatase TiO$_2$ (1 g, donated by Siant-Gobain) which was ground into powder and filtered by a sieve (mesh size 60). The surface area of the support was 34.8 m^{2}g^{-1}. The solvent was slowly evaporated in air until the sample was completely dry. The dry sample (200 mg) was calcined in the mixture of oxygen and argon (20:80 *v*/*v*) at 300 °C after increasing the temperature 5 °C min^{-1} for 1 hour, after which the temperature was decreased to 50 °C. The sample was reduced at 250 °C for 30 min in the hydrogen/argon mixture (10:80 *v*/*v*). The sample was cooled to room temperature before starting the reaction studies. Bulk Pd catalyst was prepared by mixing Pd (2 mg) with TiO$_2$ (198 mg). The sample was calcined at 1000 °C for 4 h to form large Pd and was also reduced with hydrogen at 250 °C before the catalytic reaction.

A continuous-flow packed-bed reactor (0.6 × 30 cm) was used for the activity studies. In a typical run, the volumetric flow ratios of argon, propylene, hydrogen, and oxygen were 1:1:1:1, controlled by mass flow controllers. The total flow rate was 480 mL h^{-1}. The products were analyzed by GC (SRI 8010 A), MS (SRI), and NMR spectroscopy (Varian UNITY INOVA 400 MHz). A Porapack column was used for the separation of products. Both a thermal conductivity detector and flame ionization detector were used. For NMR spectroscopic analysis, the products were collected in a CDCl$_3$ solvent cold trap.

The Pd/TiO$_2$ catalysts were imaged by HRTEM (JEOL 2010FX) to determine the morphology and size of the Pd nanoclusters. The binding energies of Pd in the Pd/TiO$_2$ catalyst were monitored by XPS (Kratos, Axis Ultra) with a monochromated Al$_{K\alpha}$ source.

Received: January 4, 2005
Revised: April 15, 2005
Published online: June 28, 2005

Keywords: benzene · heterogeneous catalysis · nanostructures · palladium · propylene coupling

---

[1] A. K. Sinha, S. Seelan, S. Tsubota, M. Haruta, *Angew. Chem.* **2004**, *116*, 1572–1574; *Angew. Chem. Int. Ed.* **2004**, *43*, 1546–1548.
[2] H.-G. Boyen, G. Kästle, F. Weigl, B. Koslowski, C. Dietrich, P. Ziemann, J. P. Spatz, S. Riethmüller, C. Hartmann, M. Möller, *Science* **2002**, *297*, 1533–1536.
[3] B. R. Cuenya, S.-H. Baeck, T. F. Jaramillo, E. W. McFarland, *J. Am. Chem. Soc.* **2003**, *125*, 12928–12934.
[4] J. Chou, N. Franklin, S.-H Baeck, T. F. Jaramillo, E. W. McFarland, *Catal. Lett.* **2004**, *95*, 107–111.
[5] G. Kästle, H.-G. Boyen, F. Weigl, G. Lengl, T. Herzog, P. Ziemann, S. Riethmüller, O. Mayer, C. Hartmann, J. P. Spatz, M. Möller, M. Ozawa, F. Banhart, M. G. Garnier, P. Oelhafen, *Adv. Funct. Mater.* **2003**, *13*, 853–861.
[6] a) C. N. Satterfield in *Heterogeneous Catalysis in Industrial Practice*, 2nd ed., McGraw-Hill, New York, **1991**, pp. 6–18; b) Y. Takasu, T. Sakuma, Y. Matsuda, *Chem. Lett.* **1985**, *8*, 1179.
[7] T. Ueno, M. Suzuki, T. Goto, T. Matsumoto, T. Nagayama, Y. Watanabe, *Angew. Chem.* **2004**, *116*, 2581–2584; *Angew. Chem. Int. Ed.* **2004**, *43*, 2527–2530.
[8] K. Murata, Y. Liu, N. Mimura, M. Inaba, *J. Catal.* **2003**, *220*, 513–518.

[9] W. Laufer, R. Meiers, W. Hölderich, *J. Mol. Catal. A* **1999**, *141*, 215–221.

[10] G. Blanco-Brieva, E. Cano-Serrano, J. M. Campos-Martin, J. L. G. Fierro, *Chem. Commun.* **2004**, 1184–1185.

[11] R. Barnes, I. M. Abdelrehim, T. E. Madey, *Top. Catal.* **2001**, *14*, 53–61.

[12] S. Abbet, U. Heiz, A. M. Ferrari, L. Giordano, C. D. Valentin, G. Pacchioni, *Thin Solid Films* **2001**, *400*, 37–42.

[13] S. Abbet, A. Sanchez, U. Heiz, W.-D. Schneider, *J. Catal.* **2001**, *198*, 122–127.

[14] K. G. Pierce, M. A. Barteau, *J. Phys. Chem.* **1994**, *98*, 3882–3892.

[15] R. L. Middleton, R. M. Lambert, *Catal. Lett.* **1999**, *59*, 15–20.

[16] A. Clotet, J. M. Ricart, F. Illas, G. Pacchioni, R. M. Lambert, *J. Am. Chem. Soc.* **2000**, *122*, 7573–7578.

[17] B. Grzybowska, J. Haber, J. Janas, *J. Catal.* **1977**, *49*, 150–163.

[18] J. F. Moulder, W. F. Stickle, P. E. Sobol, K. Bomben in *Handbook of X-Ray Photoelectron Spectroscopy* (Eds.: J. Chastain, R. C. King, Jr.), Physical Electronics, Inc. USA **1995**, pp. 118–119.

[19] J. Chou, E. W. McFarland, *Chem. Commun.* **2004**, *16*, 1648–1649.

[20] H. Fornander, L.-G. Ekedahl, H. Dannetun, *Catal. Lett.* **1999**, *59*, 107–113.

[21] A. Bielanski, J. Habe, *Oxygen in Catalysis*, Marcel Dekker, New York, **1991**, pp. 294–298.